2014 5th IEEE RAS & EMBS International Conference on
Biomedical Robotics and Biomechatronics (BioRob)
August 12-15, 2014. São Paulo, Brazil

Customized Load Cell for Three-Dimensional Force-Moment Measurements in Orthodontics

M. Mencattelli, *Student, IEEE*, E. Donati, *Student, IEEE,* M. Cultrone, C. Stefanini, *Member, IEEE*

***Abstract*— A customized load cell is developed to quantitatively evaluate the three-dimensional orthodontic actions applied during treatment. The force-torque sensor is part of a platform composed of 14 load cells, each one equipped with 6 strain gauges and interfaced with a tooth. The particular shape of the load cell allows detecting 6 mechanical actions independently that the tooth is subjected to. At the same time, a dedicated acquisition system is used to collect data simultaneously. The load cell is calibrated by applying known loads in a range between 0 N and 2 N. For each strain gauge's output, good linearity ($0.83 < R^2 < 0.99$) and great repeatability ($10^{-4}\% <$ STD $< 1.4\%$) are observed. Within this work, the load cell design, fabrication and characterization are described.**

I. Introduction

ORTHODONTICS is a medical specialty that highlights the most direct link between biomechanics and treatment outcome by applying mechanical actions to achieve tooth movement, and thus correct malocclusions. Fixed orthodontic appliances exert a three-dimensional forces-moments system on each tooth that stimulate the alveolar bone remodeling through mechanisms that are structural, mechanical and biochemical. Unfortunately, histological and clinical studies report a high incidence of irreversible damages to dental tissues during orthodontic procedures. The application of a non-biological force causes a more or less prolonged ischemia of periodontal tissue, which leads to root resorption phenomenon ([1], [2], [3], [4]). Therefore, evaluating the effective therapeutic loads is a challenging topic with regard to the improvement of orthodontic treatment strategies including the reduction of traumatic effects.

To date, several attempts have been made, ([5], [6], [7], [8], [9], [10]) but the first manufactured example of a measuring instrumentation for three-dimensional force-moment measurements occurs with Planert *et al.* [11]. Subsequently, Friederich *et al.* [12] designed a measuring system for *in vivo* detection of orthodontic loads by means of divisible special-design brackets (Fig. 1a). The brackets are able to isolate the forces from the respective tooth and introduce them into a 3D force-torque sensor by using a gripper. In another study a Robotic-Measurement-System (RMS) (Fig. 1b) was used to measure the initial forces-moments system exerted on each tooth, due to different levelling archwires [13]. The system includes a precision industrial robot RX 60 with six degrees of freedom and a force-moment sensor for quantifying single mechanical actions along the three spatial axes. The force-moment sensor holds a steel bar that carries the bracket of the tooth upon which the acting force system is to be measured. In 2009, Badawi *et al.* developed an orthodontic simulator (OSIM) to acquire 3D orthodontic actions in real time [14]. The OSIM (Fig. 1c) is a model of the human mouth consisting of one dental arch with 14 teeth on which bracket and wires are mounted. By using Industrial Automation Nano17 load cells (ATI Industrial Automation, Apex, NC), the forces-moments system was measured. A special connector that incorporates vertical and horizontal nonrotating micrometer heads has been designed to connect each tooth to a 3D load cell.

Despite these attempts over the years, there are drawbacks that cannot be ignored, such as analysis of a single tooth at a time or acquisition at a point different from that of the force application.

The advancement in miniaturized sensor technologies and software engineering inspired the developments of smart brackets: chips made with CMOS technology embedded into the bracket base. The microelectronic chips equipped with stress sensors (Fig. 2a), are able to detect the mechanical loads at different locations on the bracket. Before constructing the real smart bracket, through the design of a finite-element (FE) model, tests *in silico* are conducted to verify the proper sensor operation ([15], [16]).

Thanks to technological progress in material engineering and rapid prototyping, invisible aligners have emerged as an alternative to the common orthodontic techniques, preferred by patients because of unrestricted dietary patterns, not evident appearance and more comfort. To investigate the biomechanical effects due to therapy with invisible aligners, the methods for bracket force measurement cannot be applied: there is not enough space between teeth and aligner and the forces acting on the structure are complex. A recent study shows an alternative method to investigate the orthodontic actions on invisible aligners [17].

The authors have developed an ultra-thin piezoresistive sensor fixed on the tooth surface (Fig. 2b) to measure the three components of orthodontic forces due to invisible aligners.

However, also systems making use of microelectronic chips present the issues discussed before as long acquisition timing and increased complexity because of complex algebraic calculation to reconstruct the real measure.

M. Mencattelli (corresponding author phone: 0039-050-883010; e-mail: m.mencattelli@sssup.it), E. Donati (e-mail: e.donati@sssup.it), C. Stefanini (e-mail: cesare.stefanini@sssup.it) are with The Biorobotics Institute, Scuola Superiore Sant'Anna, Viale Rinaldo Piaggio, 34, 56025, Pontedera (Pisa), Italy.

M. Cultrone is with Studio Dentistico Cultrone, Via Ubaldesca, 14, 56025, Calcinaia (Pisa) (e-mail: oris@studiocultrone.it).

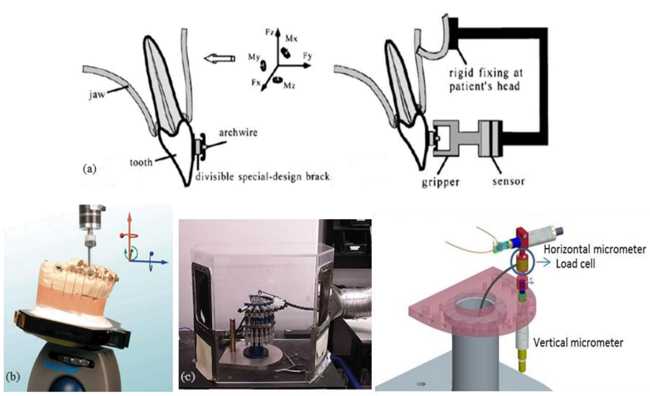

Fig. 1. Examples of measuring systems at the State of the Art. (a) divisible special-design brackets developed by [12]. (b) Robotic-Measurement-System (RMS) developed by [13]. (c) OSIM developed by [14].

Fig. 2. (a) Microelectronic chip equipped with stress sensors, developed by [15]. (b) Stress sensor chip for invisible aligners developed by [17].

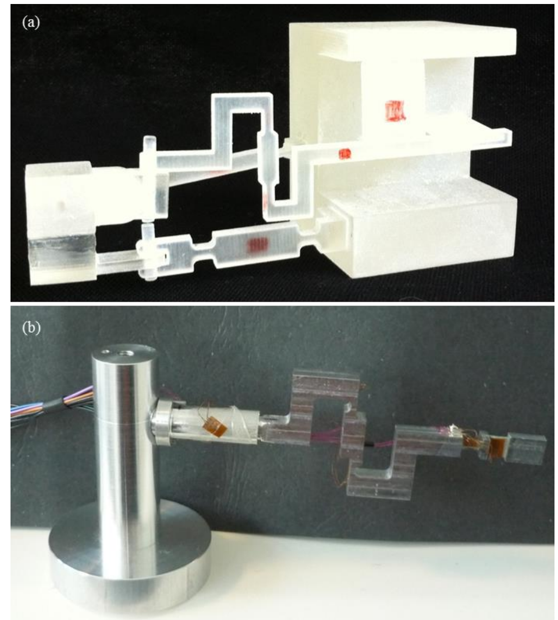

Fig. 3. (a) First prototype. (b) Second prototype of the load cell.

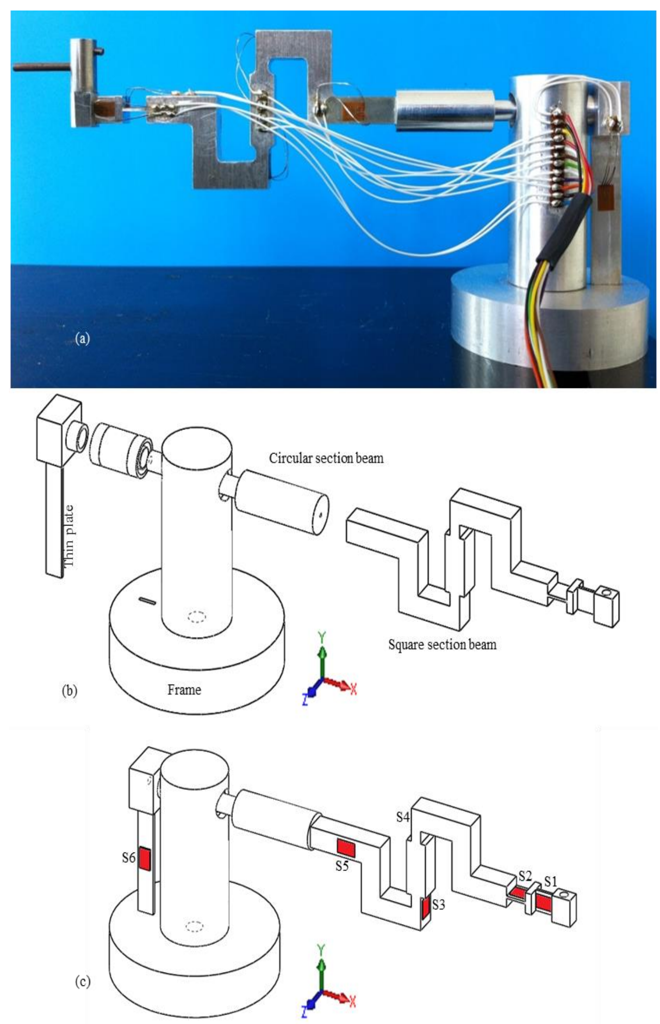

Fig. 4. (a) Customized load cell. (b) CAD exploded model. (c) CAD model with the six strain gauges marked in red.

Furthermore some tools need a long time for positioning, often the measurements are inaccurate because of the limited rigidity of the system, and the orthodontic actions cannot be simultaneously determined. Moreover, no attention has been paid to the design of measuring instrumentation suitable for all kinds of orthodontics appliances.

This study aims at designing an innovative measuring instrument that overcomes the aforementioned issues, applicable from less to more complex dental crowding cases, and usable with any type of orthodontic device. Within this work, a customized load cell, able to detect, independently and simultaneously the 3D mechanical actions exerted on the tooth by all kinds of orthodontic appliances, is presented.

II. Methods

A. Design of the Customized Load Cell

After two preliminary prototypes (Fig. 3), to optimize shape, size constrains and sensor parameters, the final customized load cell (Fig. 4a) is designed into three parts (Fig. 4b) with a variable size between 0.7 mm, in the areas where high sensitivity is required, and 10 mm in other areas. The construction material of the sensor is ergal, an aluminum alloy with better mechanical properties than aluminum itself. Six strain gauges are bonded on the load cell to allow reading the 3D mechanical actions on the tooth.

Table I shows the mechanical actions read by each strain gage (Fig. 4c) according to the reference system shown in Fig. 4. The three components consists of a frame, a circular section beam interfaced to the frame via bearings, to which a thin plate is fixed, and a square section beam. The three components are fixed together with screws in order to avoid relative movements between one another.

TABLE I. SENSORS READINGS

Strain gauges	Six mechanical actions	
	Main type of action	*Orthodontic specific nomenclature*
S1	M_y	Rotation
S2	M_z	Torque
S3	$F_x - F_y$	Lingual-buccal and extrusion-intrusion force
S4	$F_x - F_y$	Lingual-buccal and extrusion-intrusion force
S5	F_z	Mesio-distal force
S6	M_x	Tip

The six strain gauges (Micro Measurements Precision Sensors, Vishay Precision Group, Inc), (Fig. 5a) are bonded on the load cell structure by means of M-Bond 600 adhesive, after cleaning the metal surface with an abrading agent (M-Prep Conditioner A, Micro Measurements, Vishay Precision Group, Inc) and a neutralizer (M-Prep Neutralizer 5A, Micro Measurements, Vishay Precision Group, Inc). The strain gauge specifications are reported in Table II. The load cell interfaces with the tooth thanks to a dental flowable composite (Tetric EvoFlow, Ivoclar Vivadent, Inc.) commonly used in dentistry to repair teeth (Fig. 5b). This material photopolymerizes very quickly, thus allowing to position each tooth in a few seconds and that ensures high stability.
The square section beam is composed of two thin plates mutually orthogonal and divided by a rigid element. These two plates hold resistors S1 and S2 which measure respectively M_y and M_z. The strain gauges S3 and S4 are placed on the “S”-shape portion of the square section beam. Their combined reading allows measuring lingual-buccal and extrusion-intrusion forces. To understand the regions where strain is maximum, thus finding the right position to place resistors S3 and S4, a stress analysis is analytically conducted. Furthermore, to make these regions even more sensitive, their section is reduced by 50%. This is highlighted in Fig. 6 in which the stress distribution on the “S-shape” beam is simulated, with SoliWorks, by considering the structure loaded with the maximum force used during calibration (2 N). Von Mises stress distribution shows the highest sensitivity to lingual-buccal forces in the regions where S3 and S4 are placed (Fig. 6a). Regarding the response to the flexion around y- and z-axis, the two thin plates are the most affected. But, at the same time, also the areas in which S3 and S4 are bonded, are affected by F_y and F_z action (Fig. 6b).
The resistor S5 detects the force acting sagittally on the tooth. From Fig. 6c it can be seen that the area onto which S5 is attached is only partially affected by the strain. This is one of the features that have to be improved in future developments.
The bearings around the circular section beam allow the latter to rotate around its own axis (x-axis), by avoiding transmitting any other type of movement/mechanical actions. Thus, the beam rotation around x-axis results in a moment that deforms the thin plate and allowing S6 to acquire the M_x-action. This particular design allows achieving the maximum decoupling of the readings with minimum overall dimensions.
Fig. 7a shows the entire platform consisting of 14 3D printed load cell prototypes. Fig. 7b shows the real measuring platform composed of 5 load cells used in preliminary tests to evaluate the effects of three different superelastic ligations in treating a malocclusion with high maxillary canine. The sensors are arranged on a slotted base which allows their movement on a plane parallel to the ground, to adjust their position before the acquisition. The platform has also a locking system for the load cells: it ensures that loads do not act on the sensors during the assembly phase.

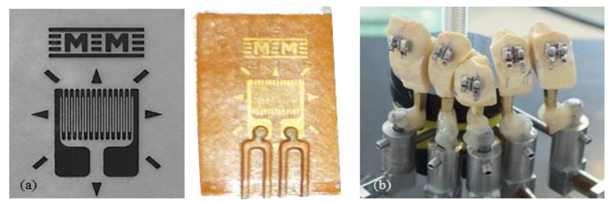

Fig. 5. (a) Micro Measurements Precision Sensors. (b) Detail of the connection between teeth and load cells by means of Tetric EvoFlow.

TABLE II

Strain gauge specifications	
Resistance (ohm)	350 ± 0.4%
Gauge factor @ 24 °C	2.12 ± 1.0%
Strain range	± 2%
Transverse sensitivity	(+1.5 ± 0.2)%
Overall dimensions (mm^2)	1.93 x 1.57
Matrix dimensions (mm^2)	5.8 x 4.1

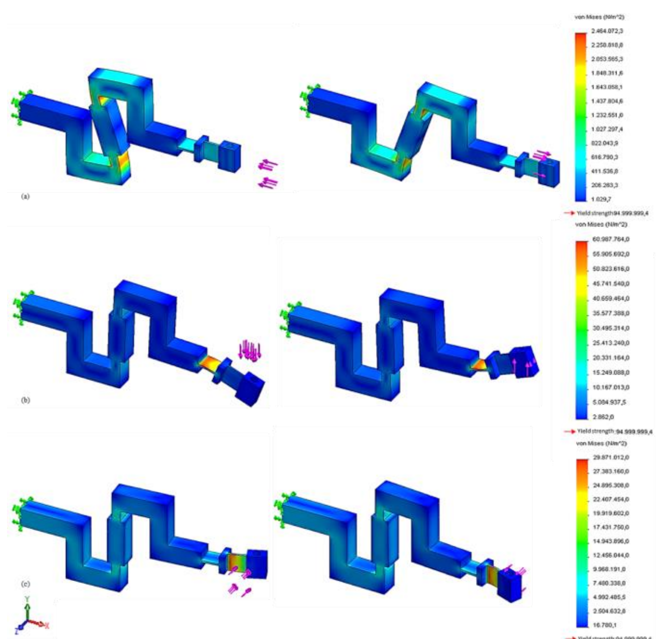

Fig. 6. (a) FEM analysis of the beam loaded with lingual-buccal force. Scale factor 24.37:1. (b) FEM analysis of the beam loaded with extrusion-intrusion force. Scale factor 1872.41:1. (c) FEM analysis of the beam loaded with mesio-distal force. Scale factor 49.59:1.

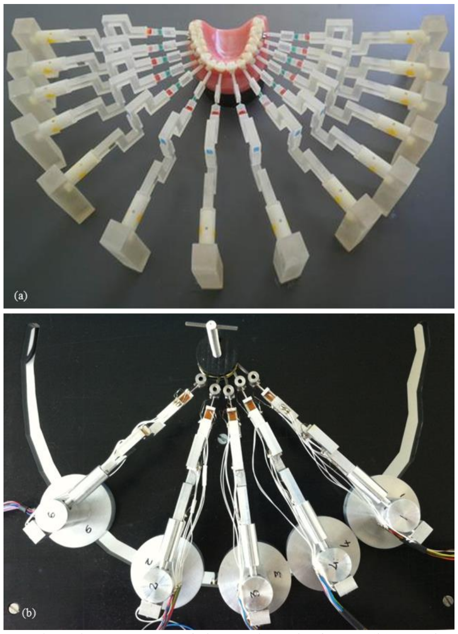

Fig. 7. (a) 3D printed prototype of the entire platform. (b) Real measuring platform with five load cells for preliminary testing.

B. Signal Conditioning and Data Acquisition

Each load cell is connected to a signal conditioning board and each board sends data to a DAQ acquisition module (NI USB X Series Multifunction DAQ) connected to a computer. The block diagram and the real signal conditioning board are shown in Fig. 8. Each of the six strain gauges of the load cell is connected into a separated electronic circuit composed by a Wheatstone bridge and an amplifier stage.

Usually, two strain gauges of the four resistors of the bridge are placed on opposite sides to decrease thermal effects. In this study, the strain gauges used are auto-thermal compensate, and therefore, one is enough to reject thermal variations. In order to verify this, some tests were performed. A single strain gauge, connected to power supply, is measured for one hour. After that time, the resistor value increased by about 0.05%. The same tests were performed on one half of the Wheatstone bridge with the same results.

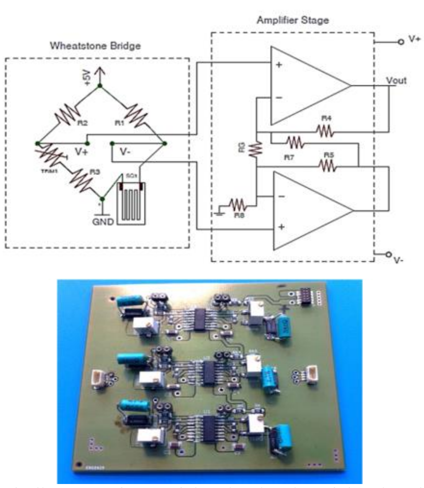

Fig. 8. (a) Block diagram of one of the six circuits of the signal conditioning board. (b) Signal conditioning board.

To avoid that thermal effects affect the readings, the experimental tests are conducted after one hour from the switching of power supply.

Opposite to the measuring resistor, a trimmer is placed to set the zero in case of voltage fluctuations due to the system.

The differential output voltage of the Wheatstone bridge is in the range of mV. To obtain an appropriate measure for the DAQ, the voltage output is amplified of 450 times. The acquisition software used is NI LabVIEW while output data are processed with MATLAB (MathWorks, Inc). The acquisition process can be started and stopped by simply turning a virtual button on the LabVIEW interface on or off, thanks to a special Virtual Instrument (VI, the LabVIEW program) which has been generated. The VI Block Diagram allows connecting the DAQ to the software, to choose which channels to acquire and to filter the signals. The VI Front Panel allows starting and stopping the measurements and to see the signals behavior during the acquisition.

III. Experimental Results

A. Sensor Calibration

The load cell was statically calibrated (Fig. 9) by applying known weights between 0 N and 2 N equally spaced of 0.05 N. The range of loads applied has been chosen according to the range on which orthodontic therapeutic loads fall [11, 18]. The weights were applied on the tip of the sensor where the tooth would be mounted during the experimental trials. Thanks to a pin extruding from the cylinder at the top of the load cell (the pin is highlighted by a red circle in Fig. 9a), the weights, contained in a sachet (Fig. 9b), are in turn attached in the same position by a hook.

The characterization process was performed in four different steps: the first one concerned the calibration of strain gauges number 2, 3 and 4 and implied the application of weight while the load cell was upright. Then the load cell was rotated on the horizontal plane for the calibration of strain gauges number 1 and 5. By leaving the sensor lying on the same plane and just moving the axis of weights application, strain gauge number 6 was calibrated. Finally the load cell was positioned upside down to calibrate strain gauges number 3 and 4 to the action of a lingual-buccal force. By combining the voltage outputs of resistor S3 and S4, the F_x - F_y actions can be independently detected. In particular when the load cell is subjected to an extrusion-intrusion force, the two strain gauges show opposite behaviors (S4 extends, S3 compresses). When a lingual-buccal force acts on the tooth, the two strain gauges respond in the same way. The sensor outputs were sampled at a frequency of 1 kHz for a period of 10 s. The average of the output voltages from each strain gauge at each known weight applied was used as static calibration points. By observing the curve fitting to first polynomial degree, it has been seen that it was not enough accurate compared to a second-order polynomial degree. The latter approximated the 40 calibration points very precisely, that it was enough to fit at best the outputs of each strain gauge (Fig. 10).

S1, S2 and S6 are the strain gauges that have to measure the moment actions, for this reason, in Fig. 11 are plotted the three voltage outputs with respect to a torque action, analytically calculated. The combined readings of S3 and S4 are plotted in Fig. 12. The strain gauges used are bidirectional, therefore, the sign of the resistors' responses, determines the direction of the force applied.

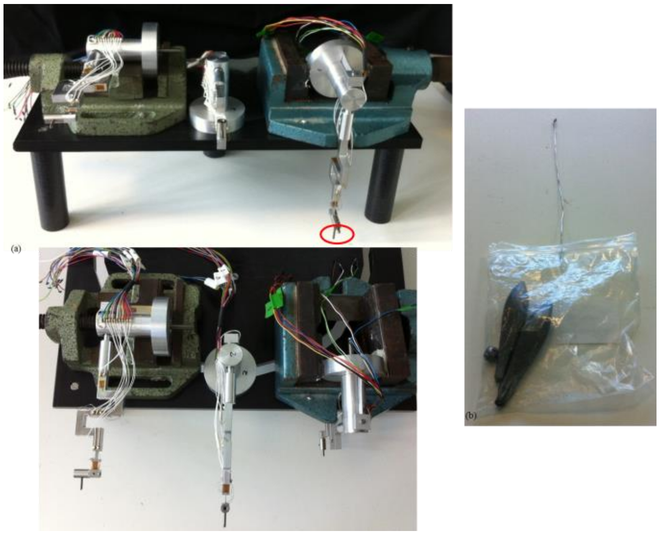

Fig. 9. (a) Experimental setup for the load cell calibration. Calibration of S1, S5 and S6 on the left. Calibration of S2, S3-S4 (for extrusion-intrusion force) at the center. Calibration of S3-S4 for lingual-buccal force on the right. (b) Known weights for the calibration.

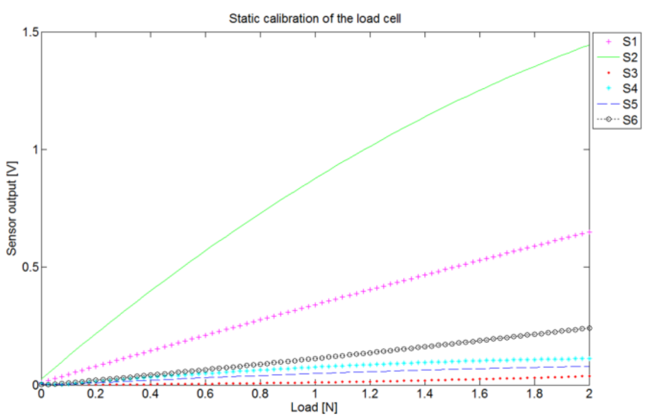

Fig. 10. Static calibration curves of the six strain gauges of the load cell.

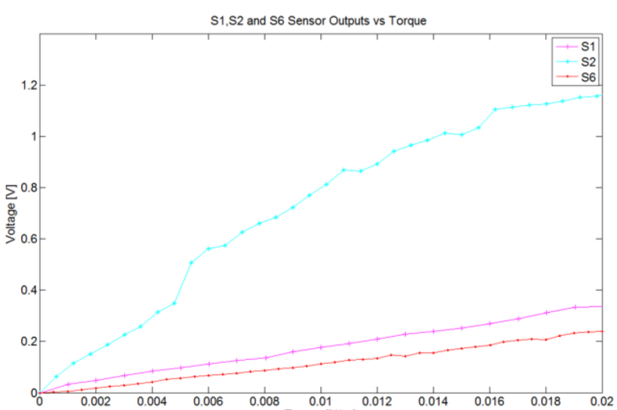

Fig. 11. S1, S2 and S6 voltage outputs with respect to a torque action.

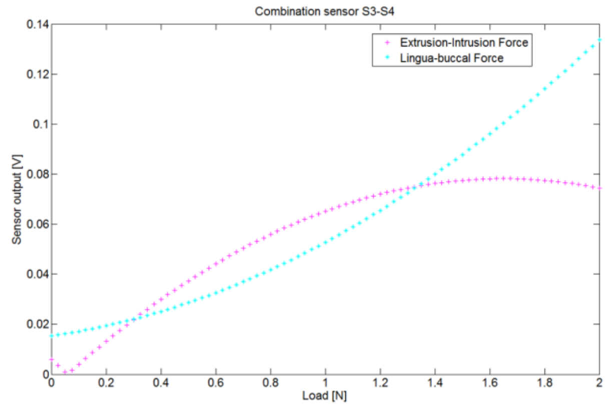

Fig. 12. Combined readings of S3 and S4.

Least squares linear regression is used to determine sensor sensitivity which is represented by the slope of the curves. It resulted in an average of 0.21V/N (S1 slope = 0.32 V/N, S2 slope = 0.7 V/N, S3 slope = 0.02 V/N, S4 slope = 0.06 V/N, S5 slope = 0.04 V/N, S6 slope = 0.12 V/N). The sensor shows a good linearity (average $R^2 = 0.91$).

B. Repeatability Tests

The experimental protocol used to calibrate the load cell was repeated to test the sensor repeatability with the difference of an interval between two weights of 0.25 N instead of 0.05 N. For each load applied, 10 repetitions were acquired. The repeatability tests were conducted with the same method, in the same laboratory by the same operator using the same equipment with short intervals of time (60 s between each repetition). The standard deviations over 10 repeated measurements, relative to their mean values, fell in the range of 0.00045% and 1.4%, thus assessing a great repeatability.

C. Inaccuracy of the System

To investigate the inaccuracy of the system, differences between two output values related to the same input, have been evaluated by applying loads from 2 N to 0 N at the end of each calibration path with the same experimental protocol previously explained. The inaccuracy is calculated as the ratio between maximum output difference for the same input, and full-scale output and it lies in a range between 0.94% and 8%.

IV. Discussion and Conclusions

Within this work, the design, fabrication and characterization of a load cell for 3D force-moment measurement in orthodontics are presented. The load cell has been successfully calibrated, by showing a good linearity for all the six strain gauges voltage outputs. Furthermore, the experimental tests showed excellent sensor repeatability. This is an important result especially for the use of the load cell. Since the sensor will be employed to investigate what happens on a tooth if subjected to orthodontic loads in static conditions, it is of paramount importance that the measuring is repeatable. The sensor sensitivity is good for the resistors S1, S2 and S6 but it results 10 times lower for resistors S3, S4 and S5. This is due to the geometry of the load cell: the areas in which these strain gauges are placed have a larger cross-section thus decreasing the sensitivity. This can be improved by lightening the structure in these areas or by changing and testing other construction materials. Also the sensor inaccuracy seems relevant (it reaches 8% of the full-scale output). Anyway, it is mainly caused by a series of external factors, such as temperature and stability of the acquisition electronics that can be better controlled in a subsequent stage to that preliminary. Finally, for a complete and deeper analysis of resistors S1, S2 and S6, the load cell should be subjected to pure torque actions to investigate their behavior and compare it with that of a mathematically deduced one, by multiplying the load applied for the correspondent lengths.

The ultimate aim of this study, as previously reported, is to realize a measurement platform composed of 14 load cells interfaced with a reconstructed anatomy of a patient. The malocclused mouth models can be obtained with a plaster cast of the real patients mouth or as 3D printed prototypes. Each tooth of the model contains a pin coming out from the bottom side by which the tooth is interfaced with a load cell. This allows acquiring measurements at radicular level. Within previous studies the measurements were performed on simulator of the human mouth (e.g. [14], thus preventing the analysis of a real pathological condition in which the teeth are touching and are crowding), or on individual teeth (e.g. [12], thus preventing to get a simultaneous overview of all the teeth). With this proposed research, the authors introduced an additional step to overcome aforementioned limitations. One of the main innovations presented lies in having developed a small device that requires real human mouth models that can be used even in cases of complex dental crowding, while maintaining the special feature of reading of forces at the point of their application. This allows avoiding the use of robotic arms and/or complex algebraic calculations (unlike what e.g. Fuck *et al.* [13] and Lapatki *et al.* [15] suggest) that make the system bulky, slows down the acquisition process and decreases the accuracy. Furthermore, the device has been designed so that it can be used to investigate the action of any type of orthodontic appliance, unlike the platforms cited at the State of the Art that are specific for one fixed orthodontics.

To date, 6 load cells are fabricated. The future steps will consist on calibrating the remaining load cells and used them to investigate three case studies treated respectively with wire-bracket complex, invisible aligners and orthodontics miniscrews. As an ultimate goal the authors aim to introduce this system as a training platform for clinicians or to develop innovative orthodontic appliances able to exert lower treatment forces.

ACKNOWLEDGMENT

The authors would like to thank Mr. Godfried Jansen Van Vuuren for his advice and support in the fabrication of measurement set-up.

REFERENCES

[1] B. Lapatki, and O. Paul, "Smart Brackets for 3D-Force-Moment Measurements in Orthodontic Research and Therapy - Developmental Status and Prospects", *Journal of Orofacial Orthopedics*, vol. 68, pp. 377-396, 2007.

[2] M. A. Casa, R. M. Faltin, K. Faltin, F. G. Sander and V. E. Arana-Chavez, "Root Resorptions in Upper First Premolars after Application of Continuous Torque Moment Intra-Individual Study", *Journal of Orofacial Orthopedics*, vol. 62, pp. 285-295, 2001.

[3] E. Chan and M. A. Darendeliler, "Physical properties of root cementum: Part 5. Volumetric analysis of root resorption craters after application of light and heavy orthodontic forces", *American Journal of Orthodontics and Dentofacial Orthopedics*, vol. 127, pp. 186–195, 2005.

[4] M. Darendeliler, O. Kharbanda, E. Chan, P. Srivicharnkul, T. Rex, M. Swain, A. Jones, and P. Petocz, "Root resorption and its association with alterations in physical properties, mineral contents and resorption craters in human premolars following application of light and heavy controlled orthodontic forces", *Orthodontics & Craniofacial Research*, vol. 7, pp. 79-97, 2004.

[5] C. J. Burstone and H. A. Koenig, "Force system from an ideal arch", *American Journal of Orthodontics*, vol. 65, pp. 270-289, 1974.

[6] D. J. Solonche, C. J. Burstone and R. A. Vanderby, "Device for Determining the Mechanical Behavior of Orthodontic Appliances", *IEEE Transactions on, Biomedical Engineering*, BME-24, pp. 538-539, 1977.

[7] C. Bourauel, D. Drescher and M. Thier, "An experimental apparatus for the simulation of three-dimensional movements in orthodontics", *Journal of Biomedical Engineering*, vol. 14, pp. 371–378, 1992.

[8] C. Menghi, J. Planert and B. Melsen, "3-D experimental identification of force systems from orthodontic loops activated for first order corrections", *The Angle Orthodontist*, vol. 69, pp. 49-57, 1999.

[9] B. Kuo, K. Takakuda and H. Miyairi, "Development of an orthodontic simulator for measurement orthodontic forces", *Journal of Medical and Dental Sciences*, vol. 48, pp. 15-21, 2001.

[10] E. Gunduz, B. U. Zachrisson, K. D. Honigl, A. G. Crismani and H. P. Bantleon, "An Improved Transpalatal Bar Design. Part I. Comparison of Moments and Forces Delivered by Two Bar Designs for Symmetrical Molar Derotation", *The Angle Orthodontist*, vol. 73, pp. 239-243, 2003.

[11] J. Planert, H. Modler, K. Ludecke and M. Eger, "A miniaturised force-torque sensor with six degrees of freedom for dental measurements" *Clinical Physics and Physiological Measurement*, vol. 13, pp. 241, 1992.

[12] D. Friedrich, N. Rosarius, G. Rau and P. Diedrich, "Measuring system for in vivo recording of force systems in orthodontic treatment-concept and analysis of accuracy", *Journal of Biomechanics*, vol. 32, pp. 81–85, 1999.

[13] L. M. Fuck and D. Drescher, "Force Systems in the Initial Phase of Orthodontic Treatment - a Comparison of Different Leveling Archwires", *Journal of Orofacial Orthopedics*, vol. 67, pp. 6-18, 2006.

[14] H. M. Badawi, R. W. Toogood, J. P. Carey, G. Heo and P. W. Major, "Three-dimensional orthodontic force measurements", *American Journal of Orthodontics and Dentofacial Orthopedics*, vol. 136, pp. 518–528, 2009.

[15] B. Lapatki, J. Bartholomeyczik, P. Ruther, I. Jonas, and O. Paul, "Smart Bracket for Multi-dimensional Force and Moment Measurement", *Journal of Dental Research*, vol. 86, pp. 73-78, 2007.

[16] S. Rues, B. Panchaphongsaphak, P. Gieschke, O. Paul and B. Lapatki, "An analysis of the measurement principle of smart brackets for 3D force and moment monitoring in orthodontics", *Journal of Biomechanics*, vol. 44, pp. 1892–1900, 2011.

[17] Y. Shi, C. Ren, W. Hao, M. Zhang, Y. Bai and Z. Wang, "An Ultra-Thin Piezoresistive Stress Sensor for Measurement of Tooth Orthodontic Force in Invisible Aligners", *IEEE, Sensors Journal*, vol. 12, pp. 1090-1097, 2012.

[18] W. R. Proffitt, H. W. Fields "The biological basis of orthodontic therapy", In: W. R. Proffitt, H. W. Fields, eds. Contemporary Orthodontics. 3rd ed. Wiesbaden: Mosby, Inc., 2000:304.